The final published version of this article is available at https://doi.org/10.1007/s00249-018-1344-9

Concentration-dependent effects of mercury and lead on Aβ42. Possible implications for Alzheimer's disease

Daniela Meleleo[1], Gabriella Notarachille[1], Vincenzo Mangini[2], Fabio Arnesano[2]

[1]Department of Biosciences, Biotechnologies and Biopharmaceutics, [2]Department of Chemistry, University of Bari "Aldo Moro", via E. Orabona 4, 70126 Bari, Italy

Running title: Effect of mercury and lead on Aβ42

Please send all correspondence to: Daniela Meleleo, via E. Orabona 4, 70126 Bari Italy, Tel: +390805442775, E-mail: danielaaddolorata.meleleo@uniba.it

Abstract

Mercury (Hg) and lead (Pb) are known to be toxic non-radioactive elements, with a well-described neurotoxicology. Much evidence supports the implication of metals as potential risk cofactors in Alzheimer's disease (AD). Although the action mechanism of the two metals remains unclear, Hg and Pb toxicity in AD could depend on their ability to favour misfolding and aggregation of amyloid beta proteins (Aβs) that seem to have toxic properties, particularly in their aggregated state. In our study, we evaluated the effect of Hg and Pb both on the Aβ42 ion channel incorporated in a planar lipid membrane made up of phosphatidylcholine containing 30% cholesterol and on the secondary structure of Aβ42 in aqueous environment. The effects of Hg and Pb on the Aβ42 peptide, observed on the channel incorporated into the membrane as well as on the peptide in solution, both decreasing Aβ42 channel frequency and in solution forming large and amorphous aggregates that are prone to precipitate, are dependent on metal concentration. These experimental data suggest that Hg and Pb interact directly with Aβs, strengthening the hypothesis that the two metals may be a risk factor in AD.

Keywords: Aβ, ion channel, lipid bilayer, aggregation, Mercury, Lead

Introduction

Alzheimer's disease (AD) is a fatal neurodegenerative disorder and the most common form of dementia. In the brain, two major hallmarks have been described, i.e. neurofibrillary tangles and senile plaques that are intracellular and extracellular protein deposits, respectively. The most important component of senile plaques is the amyloid-β (Aβ). Aβ is a 39-43 residue peptide, generated by proteolytic cleavage of amyloid precursor protein (APP) and naturally present at a very low concentration ($<10^{-8}$ M) in biological fluids (Seubert *et al.*, 1992). Aβ40 is the prevalent form, while Aβ42 is the more toxic form. Major Aβ42 toxicity is due to its high propensity to aggregate, forming oligomers and fibrillar aggregates that seem to correlate with disease progression. Aggregation of Aβ42 is faster and stronger than Aβ40, while aggregates of Aβ42 are more resistant to degradation (Hirakura *et al.*, 1999). The misfolding and aggregation of Aβ42 is a fundamental step in the pathogenesis of AD, initiating a cascade of events that finally lead to neuronal dysfunctions and death. Aβ42 aggregation is a process that, beginning from a monomer, leads to the formation of oligomers (all the way from dimers, via trimers up to oligomers of high molecular weight (200kDa). Using size-exclusion chromatography and measures of bioactivity, it is demonstrated that the high-molecular-weight forms (HMW, > 70 kDa) are predominant and relatively inactive, while the low-molecular-weight oligomers (LMW, 8-70 kDa) are less abundant and significantly more bioactive. Besides, soluble Aβ oligomers appear to be in equilibrium with fibrils of Aβ in insoluble amyloid plaques (Yang *et al.*, 2017). The results of numerous studies seem to indicate that Aβ oligomers are major neurotoxic species and are strongly correlated with disease (Lue *et al.*, 1999; Mclean *et al.*, 1999; Caughey e Lansbury, 2003; Glabe, 2006; Lesné *et al.*, 2008; Roychaudhuri *et al.*, 2009). The toxicity of oligomers has been shown with experiments both *in vivo* (Walsh *et al.*, 2002) and *in vitro* (Lambert *et al.*, 1998). In CSF samples from AD patients, concentrations of high-molecular-weight oligomers were higher than those from controls (Fukumoto *et al.*, 2010).

Because Aβ accumulation in the human brain occurs extracellularly, it is plausible to think that the cell membrane of neurons is a major target of soluble oligomers. By causing various types of damage to the cell membrane, when the soluble oligomers of Aβ cross the membrane, they can lead to intracellular changes (Laferla *et al.*, 2007; Takuma *et al.*, 2009) even as far as cell death via apoptosis (Chauhan e Chauhan, 2006; Weiner e Frenkel, 2006; Di Carlo, 2010) and/or, through direct interactions with membrane lipids, can lead to Aβ pore formation and disruption of the ion balance across the membrane (Davis e Berkowitz, 2010; Bode *et al.*, 2017). In fact, several studies indicate that the Aβ concentration at the membrane interface is higher than in the aqueous phase, and that interactions with membranes may induce fibrillogenesis (Chi *et al.*, 2008).

Metal ions are common environmental pollutants. In recent years, much experimental evidence has shown that these metal ions are involved in the pathogenesis of AD (Bush, 2000; Bocharova *et al.*, 2005; Ricchelli *et al.*, 2005; Bihaqi *et al.*, 2011; Roberts *et al.*, 2012; Bihaqi *et al.*, 2014). Several studies indicate that some metal ions can induce Aβs to precipitate, thus increasing the aggregation propensity of Aβs (Bush *et al.*, 1994a; Bush *et al.*, 1994b; Atwood *et al.*, 1998; Atwood *et al.*, 2000; Basha *et al.*, 2005a) or produce hydrogen peroxide by reducing molecular oxygen, becoming reduced after binding with Aβs (Huang *et al.*, 1999; Opazo *et al.*, 2002; Tabner *et al.*, 2002; Nelson e Alkon, 2005).

Mercury (Hg) and lead (Pb) are two environmental pollutants, known to be highly toxic elements with a well-described toxicology. Hg occurs in various forms in the environment: elemental mercury (Hg^0), inorganic mercury (Hg^+ and Hg^{2+}) and organic methyl-, ethyl-, phenyl-mercury. Each form has different solubility, reactivity and toxicity. Pb is a ubiquitous and abundant heavy metal.

Pb accumulates in three compartments: blood, soft tissues and bone, where it has an estimated half-life of 35 days in blood, of 40 days in soft tissues, of 20 to 30 years in bone. With regard to Hg, it is reported that the liver and intestinal

microflora metabolize metallic- and organic mercury-containing compounds to inorganic mercury characterized by a half-life of about 40 days.

Hg and Pb are highly poisonous, affecting different organs and organ systems (kidney and blood), most importantly the central nervous system.

Several studies have provided evidence of a link between Hg/Pb and AD, although the molecular mechanisms are unclear. Studies on concentrations of metals in plasma and cerebrospinal fluid (CSF), carried out by Gerhardsson and colleagues (Gerhardsson *et al.*, 2008), show that plasma levels of total mercury were significantly higher in subjects with AD, as well as in those with AD plus minor vascular components (AD+vasc) than in controls. No increases in mercury concentration were observed in the patients' CSF. Similar findings have been described by Mutter et al. (Mutter *et al.*, 2004; Mutter *et al.*, 2010) reporting higher mercury concentrations respectively in the brains of deceased and in the blood of living patients with AD. Experimental studies have shown that even very small concentrations of mercury may cause the nerve-cell changes typical of AD (Mutter *et al.*, 2004). Numerous studies carried out by Zawia and colleagues on latent responses to prenatal and early postnatal exposures to Pb show that exposure to Pb during development is a risk factor to promote neurodegenerative diseases supporting the hypothesis that many adult diseases have a fetal origin (Basha *et al.*, 2005b). The group of Zawia, using animal models, observed that the exposure to Pb in early life products an increase in the *APP* mRNA expression, in the activity of the transcription factor Sp1 and in Aβ levels (Wu *et al.*, 2008; Masoud *et al.*, 2016).

The results reported by Gerhardsson et al. seem to indicate that the lead concentration in CSF was significantly lower among subjects with AD and AD+vasc than in controls. However, studies of CSF metal concentrations are rather scarce, compared to studies in blood or plasma (Gerhardsson *et al.*, 2008; Park *et al.*, 2014).

The potential role for Hg and Pb toxicity in AD stems from i) strong positive correlation between blood mercury levels and CSF concentrations of Aβs (Hock *et al.*, 1998); ii) experimental studies in animals and *in vitro* reproduced the pathological signs of AD quite accurately and without any negative results (Palkiewicz *et al.*, 1994; Pendergrass *et al.*, 1997; Olivieri *et al.*, 2000; Olivieri *et al.*, 2002; Stoiber *et al.*, 2004; Kim *et al.*, 2014; Sun *et al.*, 2014); iii) mercury and lead cause protein misfolding and aggregation (Yano *et al.*, 2003; Basha *et al.*, 2005a; Tamás *et al.*, 2014).

In this work, we intend to examine the effect of Hg and Pb on the Aβ42 ion channel and therefore hypothesize that: i) Hg and Pb effect the biophysical parameters of the Aβ42 ion channel; ii) the effect of Hg and Pb on the secondary structure of Aβ42 favours the formation of molecular aggregates which are less prone to penetrate the bilayer; iii) the effects of Hg and Pb depend on the metal concentrations used. To our knowledge, this is the first study to test the effect of the two specific metals (Hg and Pb) on the Aβ42 ion channel. We carried out different experimental procedures in which the effects of Hg and Pb, at different concentrations, were evaluated on an Aβ42 ion channel incorporated into a planar lipid membrane (PLM) made up of phosphatidylcholine:cholesterol (POPC:Chol = 70:30, w/w), a composition similar to that of a neuronal membrane as well as on the secondary structure of Aβ42 in aqueous environment.

Materials and Methods

Single-channel measurement

Planar lipid membranes (PLMs) were composed of a mixture of POPC:Chol (70:30, w/w) (SIGMA) in 1% n-decane (FLUKA), prepared as previously described (Micelli *et al.*, 2004).

Bilayers were formed across a 300-μm hole in a Teflon set separating two 4000 μL Teflon chambers which held symmetrical 0.1M KCl solutions, pH=7, temperature 23±1°C. The aqueous solutions were used unbuffered. The salts used in the experiments were of analytical grade. The Müller-Rudin or painted technique (Müller *et al.*, 1962; Tien , 1974; Tien *et al.*, 1977) was used to form PLMs with lipids solubilised in n-decane. In all Aβ42 experiments performed, the conductance and capacitance of each membrane was tested by applying a voltage of ± 100mV for 15-20 minutes under stirring to ensure that the membrane was stable.

The concentration of the stock solution of Aβ42 (Sigma) was 4.6×10^{-4} M, obtained by dissolving Aβ42 powder (0.1 mg) in 48 μL of bidistilled sterile water under stirring for 3 min. From this solution, 5 μL were withdrawn and diluted in 45 μL of bidistilled sterile water under stirring for 3 min to obtain a concentration of 4.6×10^{-5} M. Both solutions were stored at -20°C until use and 4.35 μL of the second solution was added to the *cis* side of the membrane, to obtain the final concentration of 5×10^{-8} M.

Mercury chloride ($HgCl_2$) and Lead chloride ($PbCl_2$) were purchased from Sigma. Stock solutions of $HgCl_2$ or $PbCl_2$ were prepared by dissolving $HgCl_2$ or $PbCl_2$ powder (0.2715 and 0.0495 g, respectively) in 10 mL of bidistilled sterile water under stirring for 10 min to obtain a concentration of 1×10^{-1} M and 1.779×10^{-2} M, respectively. The $HgCl_2$ solutions at concentrations of 1×10^{-2}; 1×10^{-3}; 1×10^{-4} M were obtained from stock solution by scalar dilution. The $PbCl_2$ solutions at concentrations of 1.779×10^{-3}; 1.779×10^{-4} M were likewise obtained from stock solution by scalar dilution. The solutions of the two different salts were stored at 4°C until use.

In order to monitor the effect of Hg^{2+} or Pb^{2+} on the Aβ42 ion channel incorporated into PLM, after Aβ42 ion channel formation, in the open channel state, the following procedure was performed:

- in the first series of experiments, 10 μL of the different $HgCl_2$ solutions (1×10^{-1}; 1×10^{-2}; 1×10^{-3}; 1×10^{-4} M) were added to obtain the final concentration of 250, 25, 2.5, 0.25 μM, respectively on the *cis* side of the Teflon chambers, in different experimental sets;
- in the second series of experiments, 56.2 μL of the $PbCl_2$ solution at the 1.779×10^{-2} M concentration or 5.62 μL of the different $PbCl_2$ solutions (1.779×10^{-2} M; 1.779×10^{-3}; 1.779×10^{-4} M) were added to obtain the final concentration of 250, 25, 2.5, 0.25 μM, respectively on the *cis* side of the Teflon chambers, in different experimental sets.

The solutions were stirred after each addition of Aβ42 or two different salts for 1 min.

In single-channel experiments, the membrane current was monitored with an oscilloscope and recorded on a chart recorder for further analysis by hand. The *cis* and *trans* chambers were connected to the amplifier head stage by Ag/AgCl electrodes in series with a voltage source and a highly sensitive current amplifier (OPA 129). The single-channel instrumentation had a time resolution of 1-10 ms, depending on the magnitude of the single-channel conductance. The polarity of the voltage was defined according to the side where Aβ was added (the *cis* side). A trans-negative potential (indicated by a minus sign) means that a negative potential was applied to the *trans* side, the compartment opposite the one where Aβ was added.

Data analysis

Membrane capacitance was calculated using a calibration curve obtained by simulating the membrane capacitance with a discrete set of capacitances of known values, C_n, and measuring the corresponding output voltage, V_{lh}. The data obtained were fitted by the formula:

$$V_{lh} = \frac{A \times C_n}{(B + C_n)}$$

in which A and B are free parameters to be estimated by the fitting procedures. The values of parameters A and B were used to transform the V_{lh} value into capacitance data, as described by Micelli et al. (Micelli *et al.*, 2002).

The single-channel data, filtered at 300 Hz as reported by other authors (Arispe *et al.*, 1993), were obtained from at least three experiments (more than 100 single channels per experiment) performed on different days.

The Aβ42 incorporation and Hg^{2+} and Pb^{2+} action on the Aβ42 channel were studied as follows:

- To determine conductance, we measured the amplitude of channels by hand. A histogram of the conductance amplitude distribution for each experiment was constructed and fitted by a Gaussian distribution function. Results are expressed as central conductance ± standard error ($\Lambda_c \pm SE$) and were evaluated by Student t test. A value of $P < 0.05$ was considered significant. The Gaussian distribution function, Student t test and the fitting procedures were performed using the GraphPad Prism 3 software (GraphPad Prism™ version 3.0).
- To define channel lifetime, from records extending over prolonged periods, channel duration was measured considering the time between the opening and closing of each channel. The average lifetime of the conductance unit was estimated by the formula:

$$N = A_1 e^{\left(\frac{-t}{\tau_1}\right)} + A_2 e^{\left(\frac{-t}{\tau_2}\right)}$$

where N is the number of channels that remain open for a time equal to or greater than a certain time t, A_1 and A_2 are the zero time amplitudes, and τ_1 and τ_2 are related to the fast and slow components of the time constant, respectively. The single-exponential distribution is included in the formula ($A_2 = 0$). To choose between the two models, we performed an appropriate statistical test (F-test, Graph Pad Prism™ version 3.0).

- To determine the frequency (number of channels in 60 s), any detection of channel events was counted as successful. Results are expressed as frequency ± standard deviation (F±SD).

Circular dichroism measurement

Circular Dichroism (CD) measurements were performed at 28°C under a constant flow of nitrogen on a Jasco J-810 spectropolarimeter at 2.5 μM Aβ42 concentration, by using a quartz cuvette with a 1 cm optical path, a wavelength interval of 190–250 nm and 0.1 nm data pitch. All spectra, corresponding to an average of 7 scans, were baseline corrected.

One batch of Aβ42 (AlexoTech, Umeå, Sweden) was used for all studies. Salts, buffers, and ACS reagent-grade H_2O were obtained from Sigma-Aldrich (Germany).

In order to disaggregate pre-seeded Aβ42 and obtain a monomeric peptide, the starting material was treated as follows: lyophilized Aβ42 was dissolved in 10 mM NaOH, sonicated in an ice bath for 5 minutes; the pH was then adjusted to 7.3 with phosphate buffer, obtaining a final peptide stock solution of 50 μM Aβ42 in 10 mM phosphate.

An aliquot of this Aβ42 solution was diluted 10 fold with H_2O and analyzed by CD to ensure that the unaggregated, random-coil form of the peptide had been obtained.

In order to evaluate the effect of Hg^{2+} or Pb^{2+} on Aβ42 secondary structure, the peptide was incubated at different salt concentrations and analyzed by CD. Specifically, 100 μL of Aβ42 stock solution were diluted with H_2O to a final peptide

concentration of 2.5 μM and incubated alone or with 0.25, 2.5 and 25 μM $HgCl_2$ or $PbCl_2$. CD spectra were recorded after 5 min, 24 and 48 hours from sample preparation. During the incubation period, all four peptide samples were kept in quartz cuvettes with a 1 cm optical path, at 28 °C, under constant stirring at 270 r.p.m., and monitored at different time intervals by CD.

Results

Aβ42 channel activity and effect of mercury and lead on bare membrane

To test the membrane stability and to exclude the aspecific effect of the PLM, we performed control experiments with the lipid mixture only. No variation in parameters of conductance (12.7 pS) and capacitance (0.28 μF/cm^2) was observed for long period of time (over 25 hours) at applied voltages of ±80 and ±100 mV or when the bilayer was broken and withdrawn by the operator.

In all the experiments in which Aβ42 was added, before addition of the peptide, the basic conductance (12.7 pS) and capacitance (0.28 μF/cm^2) of the PLMs remained constant and no channel activity was observed, indicating that the membrane was stable. After the addition of Aβ42 (4.35 μL of the Aβ42 solution at a concentration of 4.6×10^{-5} M) to the medium facing the membrane (the *cis* side), no channel activity was observed for a period of some hours, even upon application of voltages as high as ±100 mV. In almost all the experiments, Aβ42 channel activity occurred after PLM breakage and withdrawal and only in a few experiments did channel activity occur spontaneously after a lag time of about four hours. Insertion of Aβ42 into the PLM caused a channel activity characterized by a pattern similar to that found in our previous study (Meleleo *et al.*, 2013; Notarachille *et al.*, 2014). Figure 1 shows an example of chart recordings of the Aβ42 channel activity incorporated into the PLM at the applied voltage of ±80 mV.

All single-channel events were used to calculate the channel amplitudes. All the histograms showed single-peaked conductance distributions and were fitted by a Gaussian distribution function, giving the central value of conductance (Λ_c±ES) (Stipani *et al.*, 2001; Gallucci *et al.*, 2003). Tables 1 and 2 report the central value of Λ_c±SE and the frequency values (F±SD) of Aβ42 channels, respectively, at the different applied voltages. The central conductance seems to be dependent on applied voltages decreasing as the voltage is increased and furthermore the Λ_c values are similar for negative and positive applied voltages. This behaviour had been found in our previous studies (Meleleo *et al.*, 2013; Notarachille *et al.*, 2014). The frequency values are symmetrical for negative and positive applied voltages. The values of the Aβ42 channel lifetime at different applied voltages, reported in Table 3, indicate that the channel manifests both the fast and slow lifetime components ($P<0.05$) at an applied voltage of 100mV and the slow channel lifetime component at other applied voltages.

Depending on individual susceptibility and exposure time, several studies highlight the neurotoxic effects of Hg and Pb in the concentration range of >35->200 μg/l (Hock *et al.*, 1998) and 5.6->100 μg/dl (Tong *et al.*, 2000; Papanikolaou *et al.*, 2005) respectively. We wanted to test whether the two metals, used at different concentrations, could change the properties of Aβ42 channels, such as conductance, voltage-dependence and the frequency of channel formation.

First of all, to exclude any non-specific and destabilizing effects of Hg^{2+} or Pb^{2+} *per se* on the PLMs used, we performed experiments by adding Hg^{2+} or Pb^{2+} to the medium facing the membrane. In many different experiments, the addition of Pb^{2+}, at any concentration, did not cause destabilization and breakage of the membrane, while the addition of Hg^{2+}, over the range of concentrations used in the present work, soon led to breakage of the membrane. A second membrane was

immediately formed by painting the lipid solution present around the hole, while conductance and capacitance were monitored. The stability of the second PLM was tested by applying a voltage of ±100 mV for 12 hours under stirring and monitoring constant values for PLM conductance and capacitance, using the same protocol described in our previous study (Notarachille *et al.*, 2014). In the presence of both metal ions, neither conductance nor capacitance ever exceeded 12.6 pS and 0.36 μF/cm^2, respectively, and neither showed channel-like activity.

Effect of $HgCl_2$ different concentrations on Aβ42 channel activity

To test the effect of Hg^{2+} on Aβ42 channel activity, we carried out different experimental sets in which the final concentrations of the metal were 0.25, 2.5, 25 and 250 μM. After Aβ42 channel formation and during the channel openings, Hg^{2+} was added to the *cis* side of the medium facing the membrane at an applied voltage of 80 mV. In almost all the experiments, Hg^{2+} addition, at any concentration, soon led to breakage of the membrane; then, a second membrane was immediately formed and channel activity was recorded at applied voltages of ±80, ±100 mV. Figure 2 shows examples of chart recordings of Aβ42 channel activity in POPC:Chol PLMs. After different times, depending on the mercury concentration used, the metal determined a progressive decrease in Aβ42 ion channel activity, characterized by lower frequencies than the Aβ42 channel alone. In the presence of 0.25/2.5 μM Hg^{2+}, Aβ42 channel activity progressively decreased and disappeared after about 6½-7 h; channel activity could once again be induced by applying voltages of not less than ±100 mV until it completely disappeared after a mean time of about 20 h (from Aβ42 addition), even upon application of voltages as high as ±120 mV. In the presence of 25/250 μM Hg^{2+}, Aβ42 channel activity progressively decreased until it completely disappeared after a mean time of about 6/4 hours, respectively. After this time, no channel activity was found, even when applying high voltages. In addition, at the higher concentrations, there was a decrease in conductance levels.

The central values of conductance (Λ_c±SE), in the presence of scalar Hg^{2+} concentrations and at the various applied voltages, are reported in Table 1. It is worth noting that, at any mercury concentration, central conductance seems to be inversely correlated with the applied voltages and, furthermore, the Λ_c values are symmetrical for negative and positive applied voltages, indicating that the metal does not change the channel symmetry. In the presence of 0.25 and 2.5 μM Hg^{2+}, the central conductance values were not significantly different at the four applied voltages from the Aβ42 central conductance alone. At a Hg^{2+} concentration of 25 μM, the central conductance values were significantly different at the applied voltages of ± 80 mV (P=0.0072, v.s./0.0002, e.s. at 80/-80 mV, respectively; Student t test) and -100 mV (P=0.0044, v.s.; Student t test), while at the applied voltage of 100 mV the central conductance value was no different (P=1, n.s.; Student t test) from Aβ42 central conductance alone. At a Hg^{2+} concentration of 250 μM, the central conductance values were extremely different (P=0.0006, e.s./<0.0001, e.s. at 80/-80 mV, respectively; P=0.0011, v.s./<0.0001, e.s. at 100/-100 mV, respectively; Student t test) at the four applied voltages from the Aβ42 central conductance alone.

Table 2 reports the frequency values (F±SD) of Aβ42 channels at applied voltages of ±80 mV and ±100 mV for the different mercury concentrations. Frequency values seem to be lower at negative applied voltages than at positive ones. It is worth noting that, at any mercury concentration, frequency values were significantly different at the four applied voltages from the Aβ42 frequency alone, indicating that mercury decreases the turnover of the Aβ42 channel.

The lifetime of single channels is another parameter that we used to characterize the Aβ42 channel in the presence of Hg^{2+}. For this analysis, single-channel current recordings with no less than 200 individual channels were analysed to

obtain cumulative open-state lifetime distributions, as reported in Table 3. The number of channels is not conspicuous enough to provide a reliable analysis of open-time distribution at negative applied voltages when Aβ42 + 250 μM Hg^{2+} are present in the medium facing the membrane.

Effect of $PbCl_2$ different concentrations on Aβ42 channel activity

In other experimental sets, we wanted to test the effect of scalar Pb^{2+} concentrations (0.25, 2.5, 25 and 250 μM) on Aβ42 channel activity. When the Aβ42 channels fluctuated in the open state, Pb^{2+} was added to the *cis* side of the medium facing the membrane at an applied voltage of 80 mV. In this series, the addition of Pb, at any concentration, did not cause destabilization and breakage of the membrane. Similarly, to the Hg^{2+} experimental sets, the channel conductance was monitored at applied voltages of ±80 mV and ±100 mV. Figure 3 shows examples of chart recordings of Aβ42 channel activity in POPC:Chol PLMs.

The addition of 0.25, 2.5, 25 μM Pb^{2+} to the medium facing the membrane did not produce changes in the Aβ42 ion channel conductance levels or frequency compared with those of Aβ42 alone. By contrast, the addition of 250 μM Pb^{2+} determined a progressive decrease in Aβ42 ion channel activity, characterized by lower conductance levels and frequencies than the Aβ42 channel alone. Depending on the lead concentration used, Aβ42 channel activity disappeared completely after 18, 10, 5 and 3 hours in the presence of 0.25, 2.5, 25 and 250 μM Pb^{2+}, respectively, even upon application of voltages as high as ±120 mV for two hours.

Table 1 reports the central value of Λ_c±SE of Aβ42 channels in the presence of scalar Pb^{2+} concentrations at the different applied voltages. Central conductance values, no matter which Pb concentration in the medium, seem to be dependent on applied voltages decreasing as the voltage is increased, and furthermore the Λ_c values are symmetrical for negative and positive applied voltages, indicating that Pb^{2+} also does not change the channel symmetry. In the presence of 0.25, 2.5 and 25 μM Pb^{2+}, the central conductance values were not significantly different at the four applied voltages from the Aβ42 central conductance alone. At the Pb^{2+} concentration of 250 μM, the central conductance values were extremely different ($P<0.0001$ at all applied voltages, Student t test) at the four applied voltages from the Aβ42 central conductance alone.

The frequency values (F±SD) of Aβ42 channels, in the concentration range of 0.25-25 μM Pb^{2+}, are similar to the Aβ42 frequency values alone at each applied voltage, suggesting that this Pb^{2+} concentration range does not affect channel turnover. In the presence of 250 μM Pb^{2+}, frequency values are no different to those of Aβ42 alone at applied voltages of ±80mV whereas at applied voltages of ±100mV, frequency values are halved compared to Aβ42 frequency values alone (Table 2).

Similarly, to the Hg^{2+} experiments and assuming the same conditions (no less than 200 individual channels), the lifetime analysis was performed, as reported in Table 3.

The prevalence of dual channel populations, at all applied voltages, obtained in the presence of 0.25 μM Pb^{2+} indicates a greater stability of the Aβ42 channel than under all other experimental conditions.

Effect of $HgCl_2$ and $PbCl_2$ on Aβ42 secondary structure

To test whether Hg or Pb ions modify the secondary structure of Aβ42, CD experiments using Aβ42 samples in the absence and in the presence of the two metal ions were carried out. Figures 4 and 5 show the CD spectra of Aβ42 without and with Hg^{2+} and Pb^{2+}, respectively.

At the starting point of each incubation, Aβ42 exhibited a CD profile with strong negative ellipticity, indicating the presence in solution of the peptide in a random-coil conformation characteristic of a monomeric state. After 24h of incubation in the above conditions, no significant change in the CD profile was observed for Aβ42 alone while, after a further 24h, a decrease in CD signal intensity and spectral changes were revealed, consistent with a β-type aggregation of the peptide (Figs. 4 and 5).

In the presence of $HgCl_2$ at 0.25 and 2.5 μM, the temporal evolution of CD spectra is similar to that of the peptide incubated in the absence of metal ions. In contrast, an immediate change in the CD profile is observed for the peptide incubated in the presence of 25 μM $HgCl_2$. In particular, a single broad band centered at ~215 nm instantly appeared, in accord with a high β-sheet content, associated with a decrease in the overall CD signal intensity. Such a decrease in intensity could be attributed to the formation of large amyloid aggregates, which may both precipitate from solution and scatter the light. In the subsequent hours of incubation, in the presence of 25 μM $HgCl_2$, the CD spectrum showed a further slight decrease in intensity without any change in the profile (Fig. 4).

CD spectra of Aβ42 in the presence of $PbCl_2$ up to a concentration of 25 μM showed a temporal evolution similar to that of the peptide incubated in the absence of metal ions (Fig. 5). Instead, the addition of 250 μM $HgCl_2$ or $PbCl_2$ caused considerable scattering of the solution (which contains 10 mM phosphate buffer), indicating the appearance of insoluble particles that disturb spectroscopic measurements. Such behaviour could be a result of the very low solubility of mercury or lead phosphate salts.

Thus, while the addition of $HgCl_2$ at 25 μM concentration can rapidly induce a secondary structure transition of Aβ42 from random-coil to a β conformation typical of amyloid aggregates, $PbCl_2$ is ineffective up to a concentration of 250 μM, whereas, in the presence of 250 μM Pb^{2+}, light scattering is observed in CD spectra after 5 minutes and subsequent hours of incubation (data not shown).

In both cases, at low salt concentrations (0.25 and 2.5 μM $HgCl_2$ or $PbCl_2$), the amyloidogenic process (from oligomers to fibrils) is not significantly modified by dissolved metal ions, i.e. the Aβ42 peptide aggregates slowly over time, assuming a β conformation after 48 hours of incubation under our selected conditions.

Discussion

In the last two decades, numerous studies have shown a link between AD and Hg or Pb; epigenetic studies have shown that developmental exposure of mice and primates to Pb resulted in a delayed overexpression of AD-related genes (Wu *et al.*, 2008) and in a latent increase in AD-related proteins and cognitive deficit (Eid *et al.*, 2016), while epidemiological studies have shown higher levels of Hg in the cerebral tissue of patients with Alzheimer's disease than in healthy subjects. Hg blood concentration in living patients with AD was twice as high as that of depressed patients and patients without psychiatric disorders. Besides, correlation with blood mercury concentration and Aβ in the cerebrospinal fluid was significant (Mutter *et al.*, 2004).

Mercury and lead are highly toxic to humans. Hg exposure occurs mainly through ingestion and its toxicity is caused by both acute (≥ 200 μg/L) and chronic (0-35 μg/L) exposure (Hock *et al.*, 1998). Pb exposure, especially in its inorganic form, occurs mainly through inhalation and ingestion and its toxicity is caused by both acute (≥ 100 μg/dL) (Papanikolaou *et al.*, 2005) and chronic (5.6-20.2 μg/dL) exposure (Tong *et al.*, 2000).

There are several studies showing the neurotoxicity of Hg and Pb at different concentrations using cell culture models. Fujimura and colleagues have shown that Hg (methylmercury and inorganic mercury) and Pb, in the range of concentrations 10 nM - 10 μM, product neuritic degeneration and subsequent cellular death of rat cerebrocortical neurons. (Fujimura e Usuki, 2012). A study carried out by Olivieri and colleagues, utilizing SH-SY5Y neuroblastoma cells, demonstrated that exposure of cells to 180 nM $HgCl_2$ for 30 minutes induces a 30% reduction in cellular glutathione levels. Besides, $HgCl_2$ seems to induce the release of Aβ peptides (Aβ40 and Aβ42), suggesting a possible link between AD and inorganic mercury (Olivieri *et al.*, 2000). Indeed, the results obtained by Song and Choi suggest that Hg (10-1000 nM $HgCl_2$ or MeHg) induces Aβ accumulation through APP overproduction and reduction of neprilysin (NEP) (Song e Choi, 2013). Similar results were obtained by Suresh and colleagues in a research project where SH-SY5Y cells were treated with Pb^{2+} alone, in the concentration range of 0.01-10 μM, and with Aβ40 and Pb^{2+}. Cells treated with Pb^{2+} alone exhibited a significant decrease in viability and exposure of the cells to Aβ40 and Pb^{2+} showed a further reduction in viability, suggesting that the toxic effects of Aβ40 were most potent in the presence of Pb^{2+} (Suresh *et al.*, 2012). Alterations in tau hyperphosphorylation, induced by exposure to Pb (5-100 μM) in differentiated SH-SY5Y cells, are reported by Bihaqi and colleagues (Bihaqi *et al.*, 2017).

Although the molecular mechanisms of Aβs neurotoxicity are not clear, a large body of data suggests that the primary target of amyloid peptides is the cell membrane of neurons, that may modulate the structural and functional conversion of Aβ assemblies involved in pathological processes.

Several studies have demonstrated that Aβ42 is able to interact with membrane lipids to form ion channels. Aβ42 incorporation, channel formation, channel stability and biophysical properties depend on numerous factors such as the state of assembly of the peptide, the peptide concentration and the lipid composition of the membrane. Indeed, Aβ42 is able to interact with membrane lipids forming slightly cation-selective, voltage-independent ion channels in PLMs containing anionic phospholipids (Hirakura *et al.*, 1999), exhibiting ionophore-like activity and inducing calcium influx into neurons (Simmons e Schneider, 1993) and neuron-like cells (Sanderson *et al.*, 1997). Bode and colleagues shown that Aβ42 assemblies in oligomeric preparations form voltage-independent, non-selective ion channels in membranes excised from HEK293 cells of neuronal origin (Bode *et al.*, 2017). As zwitterion lipids (PC) favour β-structure formation, they produce ion channels that are unstable (De Planque *et al.*, 2007) or have no permeation (Micelli *et al.*, 2004; Wong *et al.*, 2009). The addition of cholesterol (30% weight ratio) to a membrane made up of POPC increases the channel activity of Aβ42 and shifts its ion selectivity from cation to neutral, and oxidized cholesterol is required to produce anionic selective channels (Meleleo *et al.*, 2013). Therefore, cholesterol and its oxidation products can be considered neuroprotective factors, as the cholesterol molecule may be considered a target of Aβ42 that, by favouring insertion into the membrane, is likely to have a protective effect against fibrillation, because the balance shifts toward clearance (Meleleo *et al.*, 2013; Notarachille *et al.*, 2014).

Many factors can be involved in the initiation of Aβ aggregation from monomers to oligomeric structures. As reported in our previous study, cadmium seems to promote the aggregation process.

In the present work, the concentration-dependent effects of Hg^{2+} and Pb^{2+} on the Aβ42 ion channel and on the secondary structure of Aβ42 were evaluated. The range of concentrations of the two metals, i.e. 0.25-25 μM, corresponds to a chronic-acute dose of the metal, while the 250 μM concentration was used exclusively for experimental purposes.

The results obtained from single-channel experiments show that the central conductance values are significantly lower, at the 25 μM concentration of Hg^{2+} and are halved, at the 250 μM concentration of the metal, with respect to those of Aβ42 alone. Our results suggest that Hg^{2+} could modify Aβ molecule assembly forming the channel incorporated into the

membrane in the range of 25-250 μM concentrations. The ion channel size, depending on the peptide molecule assembly, can be calculated by means of conductance values and assuming the channel to be a water-filled hole (Notarachille *et al.*, 2014; Bode *et al.*, 2017). In this case, in POPC:Chol membranes (with an average thickness of 5 nm) and at an applied voltage of 80 mV and considering only Hg^{2+} concentrations of 25 and 250 μM, the channel diameter of AβP1-42/ Aβ42 + 25 μM Hg^{2+}/ Aβ42 +250 μM Hg^{2+} was 3.86/3.45/2.73 Å, respectively. This effect may be due to the binding of Hg^{2+} to imidazole and carboxyl groups of the aminoacid residues D1, E3, D7, E11, H13 that line the Aβ42 central pore and H14, positioned at the interface between the pore and hydrophobic residues, thus obstructing the channel. Our result is supported by studies of Hg^{2+} binding to imidazole, carboxyl and thiol groups in proteins carried out by Tamás (Tamás *et al.*, 2014) and by those of molecular models that explain the blocking effect of some metal ions on the Aβ42 channel, as carried out by Shafrir and colleagues (Shafrir *et al.*, 2010). Also, the results obtained by Minicozzi and colleagues indicate that H14 is involved in forming Aβ42 binding sites for Zn^{2+} in solubilised Aβ42 monomers (Minicozzi *et al.*, 2008).

Our results show that frequency decreases significantly compared with Aβ42 alone, as the Hg^{2+} concentration increases until the channel is blocked. Hg^{2+} is able to influence Aβ42 channel turnover until channel activity completely disappears, suggesting that the metal affects the Aβ42 molecule in the solution of the medium facing the membrane. This result is in line with that obtained by CD experiments. The secondary structure transition of the peptide from random-coil to β-sheet, induced by 25 μM Hg^{2+} addition, confirms the formation of β-structures, typical of amyloid aggregates. The decrease in CD signal intensity for Aβ42 incubated with Hg^{2+} at concentrations above 0.25 μM (i.e. 2.5 and 25 μM), could indicate the formation of large amorphous aggregates. As found by Tamás, Hg^{2+} forms stable polydendate complexes binding to imidazole, carboxyl and thiol groups of two polypeptide chains with a tetrahedral or octahedral geometry (Tamás *et al.*, 2014). This mechanism may explain the folding or refolding inhibition of proteins in vitro by heavy metal ions favouring the aggregation process of the proteins and peptides.

Regarding Pb^{2+}, the results obtained from single-channel experiments demonstrate that the metal ion, in the concentration range of 0.25-25 μM, does not modify the conductance and frequency values of an Aβ42 channel incorporated into the membrane compared to those of Aβ42 alone. On the other hand, the central conductance value is significantly lower at all applied voltages than that of Aβ42 alone when the Pb^{2+} concentration is 250 μM. This suggests that Pb^{2+} could modify Aβ molecule assembly forming the channel incorporated into the membrane. Similarly, to the Hg^{2+} experiments and assuming the same conditions (thickness of bilayer and equivalent conductivity of ions) the channel diameter values, obtained at an applied voltage of 80 mV and considering only Aβ42 and Aβ42 +250 μM Pb^{2+}, were 3.86 and 2.90 Å, respectively. These results indicate that, like Hg^{2+}, Pb^{2+} could bind to the imidazole rings and carboxyl groups of the aminoacid residues that line the pore, forming a cap. The frequency values, obtained at a concentration of 250 μM, were lower than that of Aβ42 alone at applied voltages of ±100 mV, suggesting that the metal affects channel turnover until channel activity completely disappears. To test the effect of Pb^{2+} on the peptide molecule in the solution of the medium facing the membrane, the secondary structure of Aβ42 (2.5 μM) in the presence of different Pb^{2+} concentrations was evaluated in an aqueous environment. CD results indicate that, in the Pb^{2+} concentration range of 0.25-25 μM, no significant spectra profile change is evident compared to the result obtained with the peptide in the absence of the metal, suggesting that Pb^{2+} does not determine changes in the peptide aggregation progression.

Our results seem to be in line with those obtained by Tamás and colleagues, in which the dissociation equilibrium constant (Kd') values of Pb^{2+} with imidazole and carboxyl groups are higher than those obtained for Hg^{2+} (micro/millimolar and nano/micromolar, respectively), indicating that Pb^{2+} displays lower efficacy in inhibiting peptide folding than Hg^{2+}. On the other hand, Basha and colleagues showed that, at nanomolar concentrations, Pb^{2+} promotes Aβ40 aggregation whereas

Hg^{2+} has minimal effects (Basha *et al.*, 2005a). This disagreement between the results obtained by Basha and ours may depend on the different peptide and sample preparation methods. In fact, Aβ42 is more hydrophobic than Aβ40 due to small elongation (Ile-Ala) of the stretch of hydrophobic residues in the C-terminal region that increase Aβ42's tendency to aggregate and auto-assemble (Jarrett *et al.*, 1993). Besides, sample preparation is a critical step due to some factors such as pH, salt concentrations and experimental procedures, which all play an important role in Aβ aggregation and subsequently toxicity (May *et al.*, 1992).

Our results demonstrate that the effects of Hg^{2+} and Pb^{2+} on the channel conductance, turnover and secondary structure of Aβ42 depend on the concentration of the two ions. At concentrations that correspond to a chronic-acute dose of the two metals (0.25-25 μM), Hg^{2+} influences Aβ42 conductance, turnover and structure while similar effects were obtained with higher concentration of Pb^{2+}(250 μM) indicating that their toxicity may depend on the affinity of the two metal ions for the same aminoacid residues of the Aβ42 peptide. In light of this, we propose the following mechanisms to explain the toxicity of Hg^{2+}, as well as that of Pb^{2+} at higher concentrations: - Hg^{2+} exasperates the aggregation and fibrillation process, increasing the formation of β-structures and large amorphous aggregates; - Hg^{2+} inhibits a possible mechanism of clearance by which cholesterol molecules may be considered as targets of Aβ42 as they favour insertion of the peptide into the membrane, thus removing it from the fibrillation process, and thereby decreasing channel activity and turnover; - likewise, Hg^{2+} inhibits the return of membrane potential from the excitability threshold by decreasing the central conductance of the Aβ42 channel with neutral ion selectivity in POPC:Chol PLMs (Fig.6).

Our present findings support and extend the emerging concept that certain metals can be risk cofactors for AD, suggesting that they may play a significant role in the formation and neurotoxicity of Aβ fibrils or oligomers and would be useful when exploring compounds with chelation properties that may have therapeutic interest for the treatment of Alzheimer's disease.

Acknowledgments

The authors acknowledge Dr. Antonio Rosato and Maria Incoronata Nardella for their assistance in the recording of CD spectra. The University of Bari and the Consorzio Interuniversitario di Ricerca in Chimica dei Metalli nei Sistemi Biologici (CIRCMSB) are gratefully acknowledged for their support for this work.
The authors acknowledge Anthony Green for proofreading and providing linguistic advice.

Conflict of interest: The authors declare that they do not have a conflict of interest.

References

Arispe, N., E. Rojas and H. Pollard (1993). "Alzheimer disease amyloid beta protein forms calcium channels in bilayer membranes: blockade by tromethamine and aluminum." Proc Natl Acad Sci U S A **90**(2): 567-571.

Atwood, C., R. Moir, X. Huang, R. Scarpa, N. Bacarra, D. Romano, M. Hartshorn, R. Tanzi and A. Bush (1998). "Dramatic aggregation of Alzheimer abeta by Cu(II) is induced by conditions representing physiological acidosis." J Biol Chem **273**(21): 12817-12826.

Atwood, C. S., R. C. Scarpa, X. Huang, R. D. Moir, W. D. Jones, D. P. Fairlie, R. E. Tanzi and A. I. Bush (2000). "Characterization of copper interactions with alzheimer amyloid beta peptides: identification of an attomolar-affinity copper binding site on amyloid beta1-42." J Neurochem **75**(3): 1219-1233.

Basha, M. R., M. Murali, H. K. Siddiqi, K. Ghosal, O. K. Siddiqi, H. A. Lashuel, Y. W. Ge, D. K. Lahiri and N. H. Zawia (2005a). "Lead (Pb) exposure and its effect on APP proteolysis and Abeta aggregation." FASEB J **19**(14): 2083-2084.

Basha, M. R., W. Wei, S. A. Bakheet, N. Benitez, H. K. Siddiqi, Y. W. Ge, D. K. Lahiri and N. H. Zawia (2005b). "The fetal basis of amyloidogenesis: exposure to lead and latent overexpression of amyloid precursor protein and beta-amyloid in the aging brain." J Neurosci **25**(4): 823-829.

Bihaqi, S. W., A. Bahmani, G. M. Subaiea and N. H. Zawia (2014). "Infantile exposure to lead and late-age cognitive decline: relevance to AD." Alzheimers Dement **10**(2): 187-195.

Bihaqi, S. W., A. Eid and N. H. Zawia (2017). "Lead exposure and tau hyperphosphorylation: An in vitro study." Neurotoxicology **62**: 218-223.

Bihaqi, S. W., H. Huang, J. Wu and N. H. Zawia (2011). "Infant exposure to lead (Pb) and epigenetic modifications in the aging primate brain: implications for Alzheimer's disease." J Alzheimers Dis **27**(4): 819-833.

Bocharova, O. V., L. Breydo, V. V. Salnikov and I. V. Baskakov (2005). "Copper(II) inhibits in vitro conversion of prion protein into amyloid fibrils." Biochemistry **44**(18): 6776-6787.

Bode, D. C., M. D. Baker and J. H. Viles (2017). "Ion Channel Formation by Amyloid-β42 Oligomers but Not Amyloid-β40 in Cellular Membranes." J Biol Chem **292**(4): 1404-1413.

Bush, A. (2000). "Metals and neuroscience." Curr Opin Chem Biol **4**(2): 184-191.

Bush, A. I., W. H. Pettingell, G. Multhaup, M. d Paradis, J. P. Vonsattel, J. F. Gusella, K. Beyreuther, C. L. Masters and R. E. Tanzi (1994a). "Rapid induction of Alzheimer A beta amyloid formation by zinc." Science **265**(5177): 1464-1467.

Bush, A. I., W. H. Pettingell, M. D. Paradis and R. E. Tanzi (1994b). "Modulation of A beta adhesiveness and secretase site cleavage by zinc." J Biol Chem **269**(16): 12152-12158.

Caughey, B. and P. T. Lansbury (2003). "Protofibrils, pores, fibrils, and neurodegeneration: separating the responsible protein aggregates from the innocent bystanders." Annu Rev Neurosci **26**: 267-298.

Chauhan, V. and A. Chauhan (2006). "Oxidative stress in Alzheimer's disease." Pathophysiology **13**(3): 195-208.

Chi, E. Y., C. Ege, A. Winans, J. Majewski, G. Wu, K. Kjaer and K. Y. Lee (2008). "Lipid membrane templates the ordering and induces the fibrillogenesis of Alzheimer's disease amyloid-beta peptide." Proteins **72**(1): 1-24.

Davis, C. H. and M. L. Berkowitz (2010). "A molecular dynamics study of the early stages of amyloid-beta(1-42) oligomerization: the role of lipid membranes." Proteins **78**(11): 2533-2545.

de Planque, M. R., V. Raussens, S. A. Contera, D. T. Rijkers, R. M. Liskamp, J. M. Ruysschaert, J. F. Ryan, F. Separovic and A. Watts (2007). "beta-Sheet structured beta-amyloid(1-40) perturbs phosphatidylcholine model membranes." J Mol Biol **368**(4): 982-997.

Di Carlo, M. (2010). "Beta amyloid peptide: from different aggregation forms to the activation of different biochemical pathways." Eur Biophys J **39**(6): 877-888.

Eid, A., S. W. Bihaqi, W. E. Renehan and N. H. Zawia (2016). "Developmental lead exposure and lifespan alterations in epigenetic regulators and their correspondence to biomarkers of Alzheimer's disease." Alzheimers Dement (Amst) **2**: 123-131.

Fujimura, M. and F. Usuki (2012). "Differing effects of toxicants (methylmercury, inorganic mercury, lead, amyloid β, and rotenone) on cultured rat cerebrocortical neurons: differential expression of rho proteins associated with neurotoxicity." Toxicol Sci **126**(2): 506-514.

Fukumoto, H., T. Tokuda, T. Kasai, N. Ishigami, H. Hidaka, M. Kondo, D. Allsop and M. Nakagawa (2010). "High-molecular-weight beta-amyloid oligomers are elevated in cerebrospinal fluid of Alzheimer patients." FASEB J **24**(8): 2716-2726.

Gallucci, E., D. Meleleo, S. Micelli and V. Picciarelli (2003). "Magainin 2 channel formation in planar lipid membranes: the role of lipid polar groups and ergosterol." Eur Biophys J **32**(1): 22-32.

Gerhardsson, L., T. Lundh, L. Minthon and E. Londos (2008). "Metal concentrations in plasma and cerebrospinal fluid in patients with Alzheimer's disease." Dement Geriatr Cogn Disord **25**(6): 508-515.

Glabe, C. G. (2006). "Common mechanisms of amyloid oligomer pathogenesis in degenerative disease." Neurobiol Aging **27**(4): 570-575.

Hirakura, Y., M. Lin and B. Kagan (1999). "Alzheimer amyloid abeta1-42 channels: effects of solvent, pH, and Congo Red." J Neurosci Res **57**(4): 458-466.

Hock, C., G. Drasch, S. Golombowski, F. Müller-Spahn, B. Willershausen-Zönnchen, P. Schwarz, U. Hock, J. H. Growdon and R. M. Nitsch (1998). "Increased blood mercury levels in patients with Alzheimer's disease." J Neural Transm (Vienna) **105**(1): 59-68.
Huang, X., M. P. Cuajungco, C. S. Atwood, M. A. Hartshorn, J. D. Tyndall, G. R. Hanson, K. C. Stokes, M. Leopold, G. Multhaup, L. E. Goldstein, R. C. Scarpa, A. J. Saunders, J. Lim, R. D. Moir, C. Glabe, E. F. Bowden, C. L. Masters, D. P. Fairlie, R. E. Tanzi and A. I. Bush (1999). "Cu(II) potentiation of alzheimer abeta neurotoxicity. Correlation with cell-free hydrogen peroxide production and metal reduction." J Biol Chem **274**(52): 37111-37116.
Jarrett, J. T., E. P. Berger and P. T. Lansbury (1993). "The C-terminus of the beta protein is critical in amyloidogenesis." Ann N Y Acad Sci **695**: 144-148.
Kim, D. K., J. D. Park and B. S. Choi (2014). "Mercury-induced amyloid-beta (Aβ) accumulation in the brain is mediated by disruption of Aβ transport." J Toxicol Sci **39**(4): 625-635.
LaFerla, F. M., K. N. Green and S. Oddo (2007). "Intracellular amyloid-beta in Alzheimer's disease." Nat Rev Neurosci **8**(7): 499-509.
Lambert, M., A. Barlow, B. Chromy, C. Edwards, R. Freed, M. Liosatos, T. Morgan, I. Rozovsky, B. Trommer, K. Viola, P. Wals, C. Zhang, C. Finch, G. Krafft and W. Klein (1998). "Diffusible, nonfibrillar ligands derived from Abeta1-42 are potent central nervous system neurotoxins." Proc Natl Acad Sci U S A **95**(11): 6448-6453.
Lesné, S., L. Kotilinek and K. H. Ashe (2008). "Plaque-bearing mice with reduced levels of oligomeric amyloid-beta assemblies have intact memory function." Neuroscience **151**(3): 745-749.
Lue, L., Y. Kuo, A. Roher, L. Brachova, Y. Shen, L. Sue, T. Beach, J. Kurth, R. Rydel and J. Rogers (1999). "Soluble amyloid beta peptide concentration as a predictor of synaptic change in Alzheimer's disease." Am J Pathol **155**(3): 853-862.
Masoud, A. M., S. W. Bihaqi, J. T. Machan, N. H. Zawia and W. E. Renehan (2016). "Early-Life Exposure to Lead (Pb) Alters the Expression of microRNA that Target Proteins Associated with Alzheimer's Disease." J Alzheimers Dis **51**(4): 1257-1264.
May, P. C., B. D. Gitter, D. C. Waters, L. K. Simmons, G. W. Becker, J. S. Small and P. M. Robison (1992). "beta-Amyloid peptide in vitro toxicity: lot-to-lot variability." Neurobiol Aging **13**(5): 605-607.
McLean, C., R. Cherny, F. Fraser, S. Fuller, M. Smith, K. Beyreuther, A. Bush and C. Masters (1999). "Soluble pool of Abeta amyloid as a determinant of severity of neurodegeneration in Alzheimer's disease." Ann Neurol **46**(6): 860-866.
Meleleo, D., A. Galliani and G. Notarachille (2013). "AβP1-42 incorporation and channel formation in planar lipid membranes: the role of cholesterol and its oxidation products." J Bioenerg Biomembr **45**(4): 369-381.
Micelli, S., E. Gallucci, D. Meleleo, V. Stipani and V. Picciarelli (2002). "Mitochondrial porin incorporation into black lipid membranes: ionic and gating contribution to the total current." Bioelectrochemistry **57**(2): 97-106.
Micelli, S., D. Meleleo, V. Picciarelli and E. Gallucci (2004). "Effect of sterols on beta-amyloid peptide (AbetaP 1-40) channel formation and their properties in planar lipid membranes." Biophys J **86**(4): 2231-2237.
Minicozzi, V., F. Stellato, M. Comai, M. Dalla Serra, C. Potrich, W. Meyer-Klaucke and S. Morante (2008). "Identifying the minimal copper- and zinc-binding site sequence in amyloid-beta peptides." J Biol Chem **283**(16): 10784-10792.
Mutter, J., A. Curth, J. Naumann, R. Deth and H. Walach (2010). "Does inorganic mercury play a role in Alzheimer's disease? A systematic review and an integrated molecular mechanism." J Alzheimers Dis **22**(2): 357-374.
Mutter, J., J. Naumann, C. Sadaghiani, R. Schneider and H. Walach (2004). "Alzheimer disease: mercury as pathogenetic factor and apolipoprotein E as a moderator." Neuro Endocrinol Lett **25**(5): 331-339.
Müller, P., D. Rudin, T. Tien and W. Weacott (1962). "Reconstitution of cell membrane structure in vitro and its trasformation into an excitable system." Nature **194**: 979-980.
Nelson, T. J. and D. L. Alkon (2005). "Oxidation of cholesterol by amyloid precursor protein and beta-amyloid peptide." J Biol Chem **280**(8): 7377-7387.
Notarachille, G., F. Arnesano, V. Calò and D. Meleleo (2014). "Heavy metals toxicity: effect of cadmium ions on amyloid beta protein 1-42. Possible implications for Alzheimer's disease." Biometals **27**(2): 371-388.
Olivieri, G., C. Brack, F. Müller-Spahn, H. B. Stähelin, M. Herrmann, P. Renard, M. Brockhaus and C. Hock (2000). "Mercury induces cell cytotoxicity and oxidative stress and increases beta-amyloid secretion and tau phosphorylation in SHSY5Y neuroblastoma cells." J Neurochem **74**(1): 231-236.
Olivieri, G., M. Novakovic, E. Savaskan, F. Meier, G. Baysang, M. Brockhaus and F. Müller-Spahn (2002). "The effects of beta-estradiol on SHSY5Y neuroblastoma cells during heavy metal induced oxidative stress, neurotoxicity and beta-amyloid secretion." Neuroscience **113**(4): 849-855.
Opazo, C., X. Huang, R. A. Cherny, R. D. Moir, A. E. Roher, A. R. White, R. Cappai, C. L. Masters, R. E. Tanzi, N. C. Inestrosa and A. I. Bush (2002). "Metalloenzyme-like activity of Alzheimer's disease beta-amyloid. Cu-dependent catalytic conversion of dopamine, cholesterol, and biological reducing agents to neurotoxic H(2)O(2)." J Biol Chem **277**(43): 40302-40308.
Palkiewicz, P., H. Zwiers and F. L. Lorscheider (1994). "ADP-ribosylation of brain neuronal proteins is altered by in vitro and in vivo exposure to inorganic mercury." J Neurochem **62**(5): 2049-2052.
Papanikolaou, N. C., E. G. Hatzidaki, S. Belivanis, G. N. Tzanakakis and A. M. Tsatsakis (2005). "Lead toxicity update. A brief review." Med Sci Monit **11**(10): RA329-336.

Park, J. H., D. W. Lee, K. S. Park and H. Joung (2014). "Serum trace metal levels in Alzheimer's disease and normal control groups." Am J Alzheimers Dis Other Demen **29**(1): 76-83.
Pendergrass, J. C., B. E. Haley, M. J. Vimy, S. A. Winfield and F. L. Lorscheider (1997). "Mercury vapor inhalation inhibits binding of GTP to tubulin in rat brain: similarity to a molecular lesion in Alzheimer diseased brain." Neurotoxicology **18**(2): 315-324.
Ricchelli, F., D. Drago, B. Filippi, G. Tognon and P. Zatta (2005). "Aluminum-triggered structural modifications and aggregation of beta-amyloids." Cell Mol Life Sci **62**(15): 1724-1733.
Roberts, B. R., T. M. Ryan, A. I. Bush, C. L. Masters and J. A. Duce (2012). "The role of metallobiology and amyloid-β peptides in Alzheimer's disease." J Neurochem **120 Suppl 1**: 149-166.
Roychaudhuri, R., M. Yang, M. M. Hoshi and D. B. Teplow (2009). "Amyloid beta-protein assembly and Alzheimer disease." J Biol Chem **284**(8): 4749-4753.
Sanderson, K. L., L. Butler and V. M. Ingram (1997). "Aggregates of a beta-amyloid peptide are required to induce calcium currents in neuron-like human teratocarcinoma cells: relation to Alzheimer's disease." Brain Res **744**(1): 7-14.
Seubert, P., C. Vigo-Pelfrey, F. Esch, M. Lee, H. Dovey, D. Davis, S. Sinha, M. Schlossmacher, J. Whaley and C. Swindlehurst (1992). "Isolation and quantification of soluble Alzheimer's beta-peptide from biological fluids." Nature **359**(6393): 325-327.
Shafrir, Y., S. Durell, N. Arispe and H. R. Guy (2010). "Models of membrane-bound Alzheimer's Abeta peptide assemblies." Proteins **78**(16): 3473-3487.
Simmons, M. A. and C. R. Schneider (1993). "Amyloid beta peptides act directly on single neurons." Neurosci Lett **150**(2): 133-136.
Song, J. W. and B. S. Choi (2013). "Mercury induced the Accumulation of Amyloid Beta (Aβ) in PC12 Cells: The Role of Production and Degradation of Aβ." Toxicol Res **29**(4): 235-240.
Stipani, V., E. Gallucci, S. Micelli, V. Picciarelli and R. Benz (2001). "Channel formation by salmon and human calcitonin in black lipid membranes." Biophys J **81**(6): 3332-3338.
Stoiber, T., D. Bonacker, K. J. Böhm, H. M. Bolt, R. Thier, G. H. Degen and E. Unger (2004). "Disturbed microtubule function and induction of micronuclei by chelate complexes of mercury(II)." Mutat Res **563**(2): 97-106.
Sun, L., X. L. Zhou, H. P. Yi, S. J. Jiang and H. Yuan (2014). "Lead-induced morphological changes and amyloid precursor protein accumulation in adult rat hippocampus." Biotech Histochem **89**(7): 513-517.
Suresh, C., J. Johnson, R. Mohan and C. S. Chetty (2012). "Synergistic effects of amyloid peptides and lead on human neuroblastoma cells." Cell Mol Biol Lett **17**(3): 408-421.
Tabner, B. J., S. Turnbull, O. M. El-Agnaf and D. Allsop (2002). "Formation of hydrogen peroxide and hydroxyl radicals from A(beta) and alpha-synuclein as a possible mechanism of cell death in Alzheimer's disease and Parkinson's disease." Free Radic Biol Med **32**(11): 1076-1083.
Takuma, K., F. Fang, W. Zhang, S. Yan, E. Fukuzaki, H. Du, A. Sosunov, G. McKhann, Y. Funatsu, N. Nakamichi, T. Nagai, H. Mizoguchi, D. Ibi, O. Hori, S. Ogawa, D. M. Stern, K. Yamada and S. S. Yan (2009). "RAGE-mediated signaling contributes to intraneuronal transport of amyloid-beta and neuronal dysfunction." Proc Natl Acad Sci U S A **106**(47): 20021-20026.
Tamás, M. J., S. K. Sharma, S. Ibstedt, T. Jacobson and P. Christen (2014). "Heavy metals and metalloids as a cause for protein misfolding and aggregation." Biomolecules **4**(1): 252-267.
Tien T. H. (1974). Bilayer Lipid Membrane: Theory and Practice. New York, Marcel Dekker.
Tien, T., J. Mountz and A. Martinosi (1977). Protein-lipid interaction in bilayer lipid membranes (BLM). The Enzyme of Biological Membranes. NY Plenum**:** 139-170.
Tong, S., Y. E. von Schirnding and T. Prapamontol (2000). "Environmental lead exposure: a public health problem of global dimensions." Bull World Health Organ **78**(9): 1068-1077.
Walsh, D. M., I. Klyubin, J. V. Fadeeva, W. K. Cullen, R. Anwyl, M. S. Wolfe, M. J. Rowan and D. J. Selkoe (2002). "Naturally secreted oligomers of amyloid beta protein potently inhibit hippocampal long-term potentiation in vivo." Nature **416**(6880): 535-539.
Weiner, H. and D. Frenkel (2006). "Immunology and immunotherapy of Alzheimer's disease." Nat Rev Immunol **6**(5): 404-416.
Wong, P. T., J. A. Schauerte, K. C. Wisser, H. Ding, E. L. Lee, D. G. Steel and A. Gafni (2009). "Amyloid-beta membrane binding and permeabilization are distinct processes influenced separately by membrane charge and fluidity." J Mol Biol **386**(1): 81-96.
Wu, J., M. R. Basha, B. Brock, D. P. Cox, F. Cardozo-Pelaez, C. A. McPherson, J. Harry, D. C. Rice, B. Maloney, D. Chen, D. K. Lahiri and N. H. Zawia (2008). "Alzheimer's disease (AD)-like pathology in aged monkeys after infantile exposure to environmental metal lead (Pb): evidence for a developmental origin and environmental link for AD." J Neurosci **28**(1): 3-9.
Yang, T., S. Li, H. Xu, D. M. Walsh and D. J. Selkoe (2017). "Large Soluble Oligomers of Amyloid β-Protein from Alzheimer Brain Are Far Less Neuroactive Than the Smaller Oligomers to Which They Dissociate." J Neurosci **37**(1): 152-163.
Yano, K., N. Hirosawa, Y. Sakamoto, H. Katayama and T. Moriguchi (2003). "Aggregations of amyloid beta-proteins in the presence of metal ions." Toxicology Letters **144**(Supplement 1): s134.

Figure Legends

Fig.1 Aβ42 channel activity in POPC:Ch PLM. Representative traces illustrating channel activity of Aβ42 in membranes made up of POPC:Ch (70:30,w:w) recorded after an average of one hour from first channel formation, when channel activity is substantial and lasting. Applied voltage was set to 80 mV (top trace) and -80 mV (bottom trace). Experiments were performed in the presence of Aβ42 added to the *cis* side, while the aqueous phase contained 0.1 M KCl (pH 7) and T = 23±1°C

Fig.2 Aβ42 channel activity in POPC:Ch PLM in the presence of different $HgCl_2$ concentrations. Representative traces illustrate channel activity of Aβ42 in the presence of 0.25 μM, 2.5 μM, 25 μM, 250 μM of $HgCl_2$ recorded after an average of one hour from first channel formation. Applied voltage was set to 80 mV (top trace) and -80mV (bottom trace) for each experimental condition. Experiments were performed on a POPC:Ch (70:30, w:w) PLM in the presence of Aβ42 + $HgCl_2$ added to the *cis* side; the aqueous phase contained 0.1 M KCl (pH 7) and T = 23±1°C

Fig.3 Aβ42 channel activity in POPC:Ch PLM in the presence of different $PbCl_2$ concentrations. Representative traces illustrate channel activity of Aβ42 in the presence of 0.25 μM, 2.5 μM, 25 μM, 250 μM of $PbCl_2$ recorded after an average of two hours from first channel formation. Applied voltage was set to 80 mV (top trace) and -80mV (bottom trace) for each experimental condition. Experiments were performed on a POPC:Ch (70:30, w:w) PLM in the presence of Aβ42 + $PbCl_2$ added to the *cis* side; the aqueous phase contained 0.1 M KCl (pH 7) and T = 23±1°C

Fig.4 Effect of $HgCl_2$ on the Aβ42 secondary structure. Time-dependence of far-UV CD spectra of Aβ42 incubated in the absence and presence of three different concentrations of $HgCl_2$.

Fig.5 Effect of $PbCl_2$ on the Aβ42 secondary structure. Time-dependence of far-UV CD spectra of Aβ42 incubated in the absence and presence of three different concentrations of $PbCl_2$.

Fig.6 Schematic model of the $HgCl_2$ and $PbCl_2$ effect on the Aβ42 aggregation pathway. The molecular mechanisms are shown in order to explain the toxicity of Hg^{2+} and Pb^{2+} at higher concentrations (see text).

Table 1 Aβ42 channel mean conductance in POPC:Ch PLM in the absence and presence of different $HgCl_2$ and $PbCl_2$ concentrations. The central conductance ± standard error (Λ_c±SE) of the Aβ42 channel in the absence and presence of 0.25, 2.5, 25 and 250 μM of $HgCl_2$ and $PbCl_2$ added to the cis side of the membrane. The minimum and maximum number of channels considered (N) out of a total number of channels considered (N_t) was: Aβ42, 1417<N<8488, Nt=18345; [Aβ42]+[Hg^{2+}]=5×10^{-8}M+0.25μM, 199<N<1701, Nt=3417; [Aβ42]+[Hg^{2+}]=5×10^{-8}M+2.5μM, 294<N<1046, Nt=2637; [Aβ42]+[Hg^{2+}]=5×10^{-8}M+25μM, 204<N<1740, Nt=3305; [Aβ42]+[Hg^{2+}]=5×10^{-8}M+250μM, 155<N<1543, Nt=2580; [Aβ42]+[Pb^{2+}]=5×10^{-8}M+0.25μM, 423<N<1086, Nt=3484; [Aβ42]+[Pb^{2+}]=5×10^{-8}M+2.5μM, 525<N<1314, Nt=2911; [Aβ42]+[Pb^{2+}]=5×10^{-8}M+25μM, 351<N<912, Nt=2748; [Aβ42]+[Pb^{2+}]=5×10^{-8}M+250μM, 311<N<873, Nt=2901.

Table 2 Aβ42 channel frequency in POPC:Ch PLM in the absence and presence of different $HgCl_2$ and $PbCl_2$ concentrations. The frequency ± standard deviation (F±SD) of the Aβ42 channel in the absence and presence of 0.25, 2.5, 25 and 250 μM of $HgCl_2$ and $PbCl_2$ added to the *cis* side of the membrane. The minimum and maximum number of channels considered (N) out of a total number of channels considered (N_t) was reported in legend of Table 1.

Table 3 The channel lifetime of Aβ42 in POPC:Ch PLMs in the absence and presence of different $HgCl_2$ and $PbCl_2$ concentrations. The lifetime (τ) of the Aβ42 channel in the absence and presence of 0.25, 2.5, 25 and 250 μM of $HgCl_2$ and $PbCl_2$ added to the *cis* side of the membrane. The symbol – indicates that the number of channels is not conspicuous enough to provide a reliable analysis of open-time distribution. The minimum and maximum number of channels considered (N) out of a total number of channels considered (N_t) was: Aβ42, 655<N<2328, Nt=5582; [Aβ42]+[Hg^{2+}]=5×10^{-8}M+0.25μM, 151<N<736, Nt=1598; [Aβ42]+[Hg^{2+}]=5×10^{-8}M+2.5μM, 125<N<418, Nt=1032; [Aβ42]+[Hg^{2+}]=5×10^{-8}M+25μM, 315<N<646, Nt=961; [Aβ42]+[Hg^{2+}]=5×10^{-8}M+250μM, 175<N<351, Nt=526; [Aβ42]+[Pb^{2+}]=5×10^{-8}M+0.25μM, 188<N<265, Nt=917; [Aβ42]+[Pb^{2+}]=5×10^{-8}M+2.5μM, 117<N<262, Nt=683; [Aβ42]+[Pb^{2+}]=5×10^{-8}M+25μM, 105<N<242, Nt=748; [Aβ42]+[Pb^{2+}]=5×10^{-8}M+250μM, 110<N<214, Nt=627.

Table 1

Vs mV	Aβ42 Λc±SE nS	Hg^{2+} 0.25µM Λc±SE nS	Hg^{2+} 2.5µM Λc±SE nS	Hg^{2+} 25µM Λc±SE nS	Hg^{2+} 250µM Λc±SE nS	Pb^{2+} 0.25µM Λc±SE nS	Pb^{2+} 2.5µM Λc±SE nS	Pb^{2+} 25µM Λc±SE nS	Pb^{2+} 250µM Λc±SE nS
100	0.019±0.0007	0.020±0.0008	0.020±0.0007	0.019±0.0008	0.011±0.004	0.021±0.0007	0.020±0.001	0.019±0.001	0.010±0.001
80	0.030±0.001	0.028±0.0009	0.028±0.0009	0.024±0.001	0.015±0.009	0.028±0.001	0.026±0.001	0.025±0.001	0.017±0.003
-80	0.030±0.0007	0.028±0.0001	0.030±0.001	0.021±0.0007	0.013±0.002	0.030±0.001	0.026±0.001	0.026±0.001	0.016±0.004
-100	0.021±0.001	0.019±0.0003	0.021±0.0006	0.018±0.0005	0.010±0.001	0.021±0.0009	0.020±0.001	0.022±0.001	0.011±0.007

Table 2

Vs mV	Aβ42 F±SD	Hg^{2+} 0.25µM F±SD	Hg^{2+} 2.5µM F±SD	Hg^{2+} 25µM F±SD	Hg^{2+} 250µM F±SD	Pb^{2+} 0.25µM F±SD	Pb^{2+} 2.5µM F±SD	Pb^{2+} 25µM F±SD	Pb^{2+} 250µM F±SD
100	10.72±1.14	5.11±0.24	3.03±0.13	4.96±0.15	3.74±0.09	17.52±0.48	14.22±0.62	10.78±0.73	5.80±0.19
80	11.55±0.12	5.31±0.13	3.71±0.11	3.56±0.29	3.61±0.14	11.75±0.36	12.28±0.83	14.32±0.56	8.58±0.29
-80	10.23±0.21	3.26±0.10	3.97±0.14	3.91±0.27	1.63±0.11	13.49±0.43	10.33±0.51	14.11±0.63	10.24±0.42
-100	9.99±0.26	2.73±0.28	1.35±0.08	4.87±0.29	2.64±0.21	11.36±0.36	11.76±0.32	10.78±0.35	5.53±0.32

Table 3

	Aβ42		Hg^{2+} 0.25µM		Hg^{2+} 2.5µM		Hg^{2+} 25µM		Hg^{2+} 250µM		Pb^{2+} 0.25µM		Pb^{2+} 2.5µM		Pb^{2+} 25µM		Pb^{2+} 250µM	
Vs mV	τ_1 s	τ_2 s	τ_1 s	τ_2 s	τ_1 s	τ_2 s	τ_1 s	τ_2 s	τ_1 s	τ_2 s	τ_1 s	τ_2 s	τ_1 s	τ_2 s	τ_1 s	τ_2 s	τ_1 s	τ_2 s
100	0.19	0.97	0.68	4.22	0.41	4.32	0.97	5.69	0.37		0.22	3.94	0.80	5.90	0.33		0.33	0.98
80	0.84		1.47		1.38		1.35	6.25	0.56		0.29	2.36	1.61		1.39		0.90	
-80	1.42		0.90		1.21		-	-	-	-	0.85	6.94	1.22		0.82		0.44	
-100	1.18		0.44	4.19	1.20		-	-	-	-	0.16	2.32	1.13	5.55	0.54	5.14	0.25	

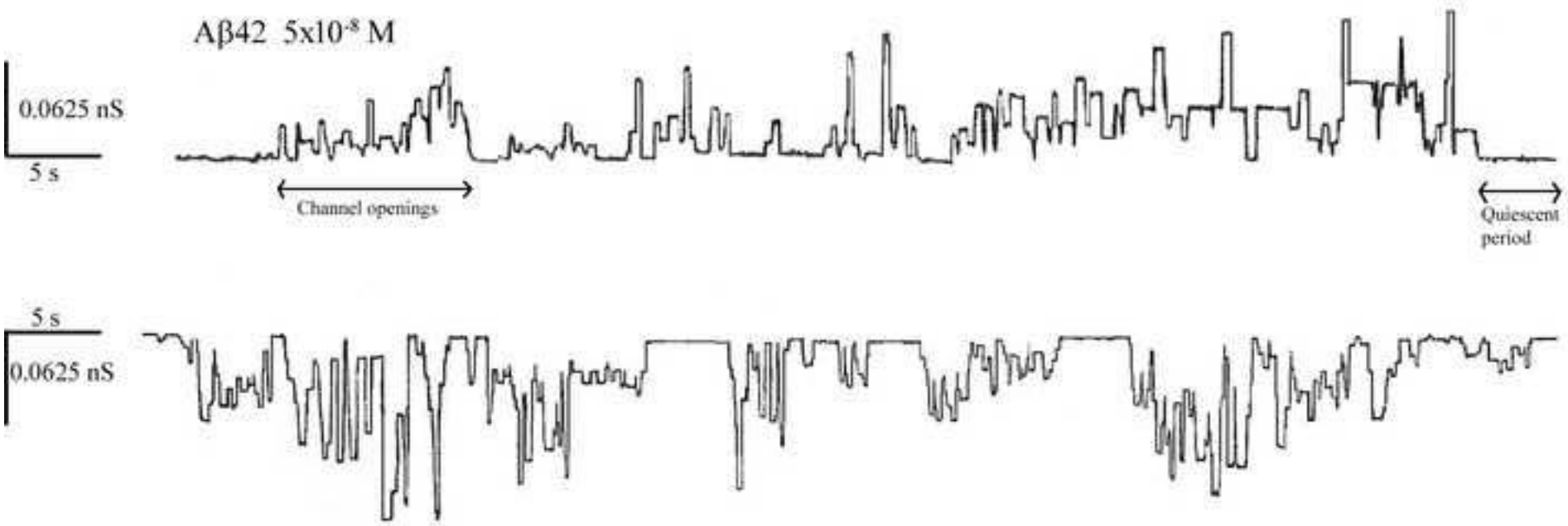

Fig.1

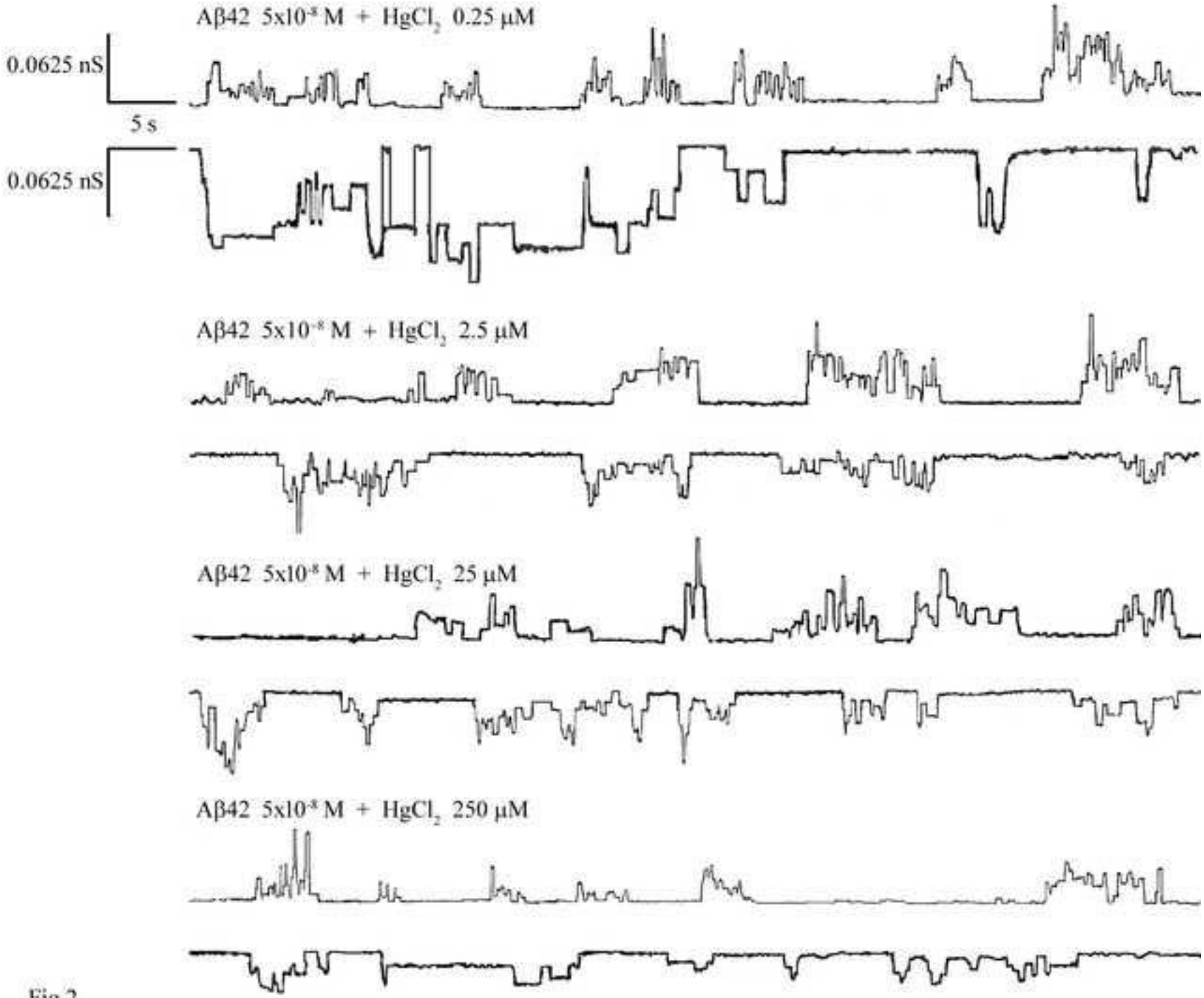

Fig.2

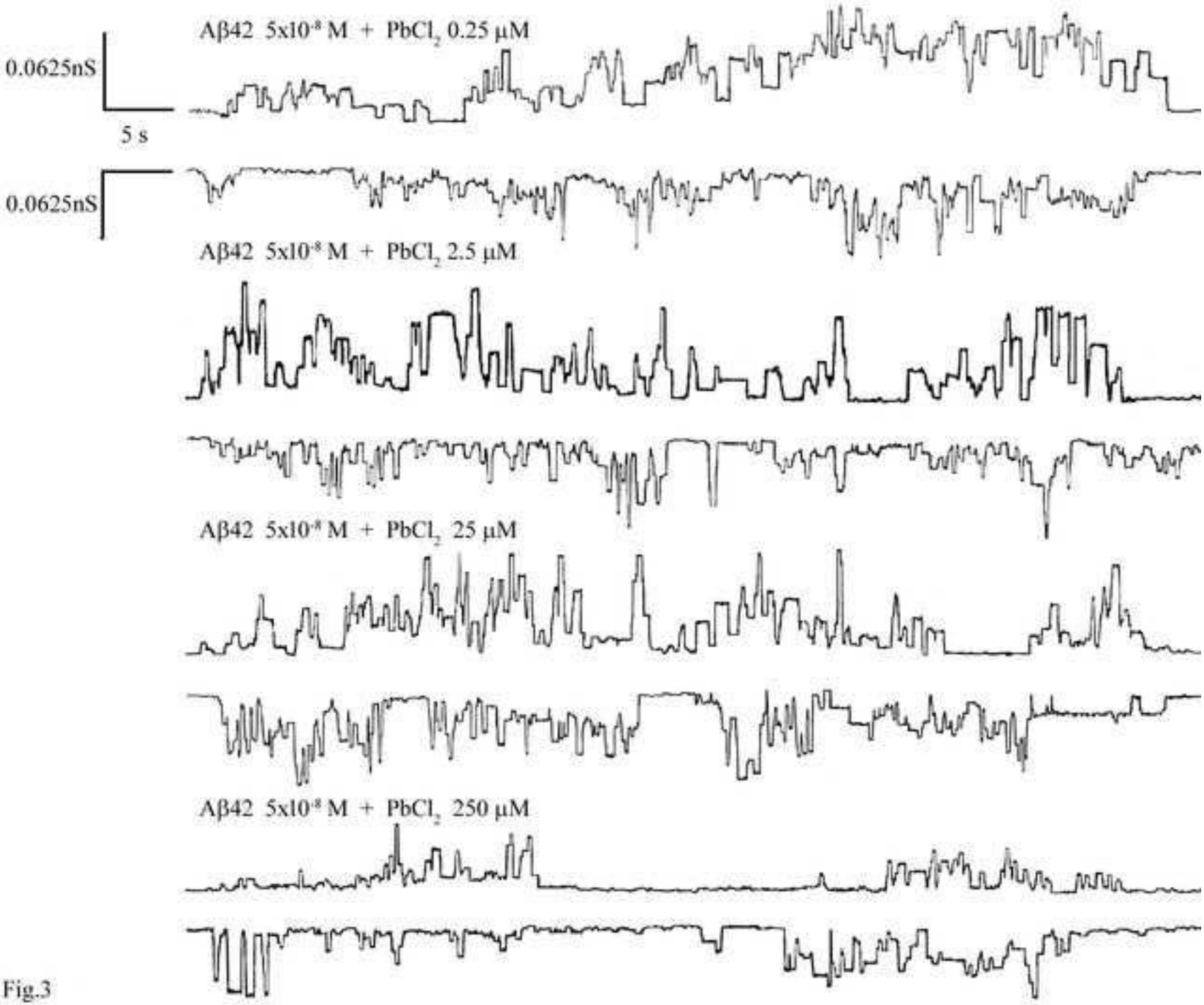

Fig.3

Images

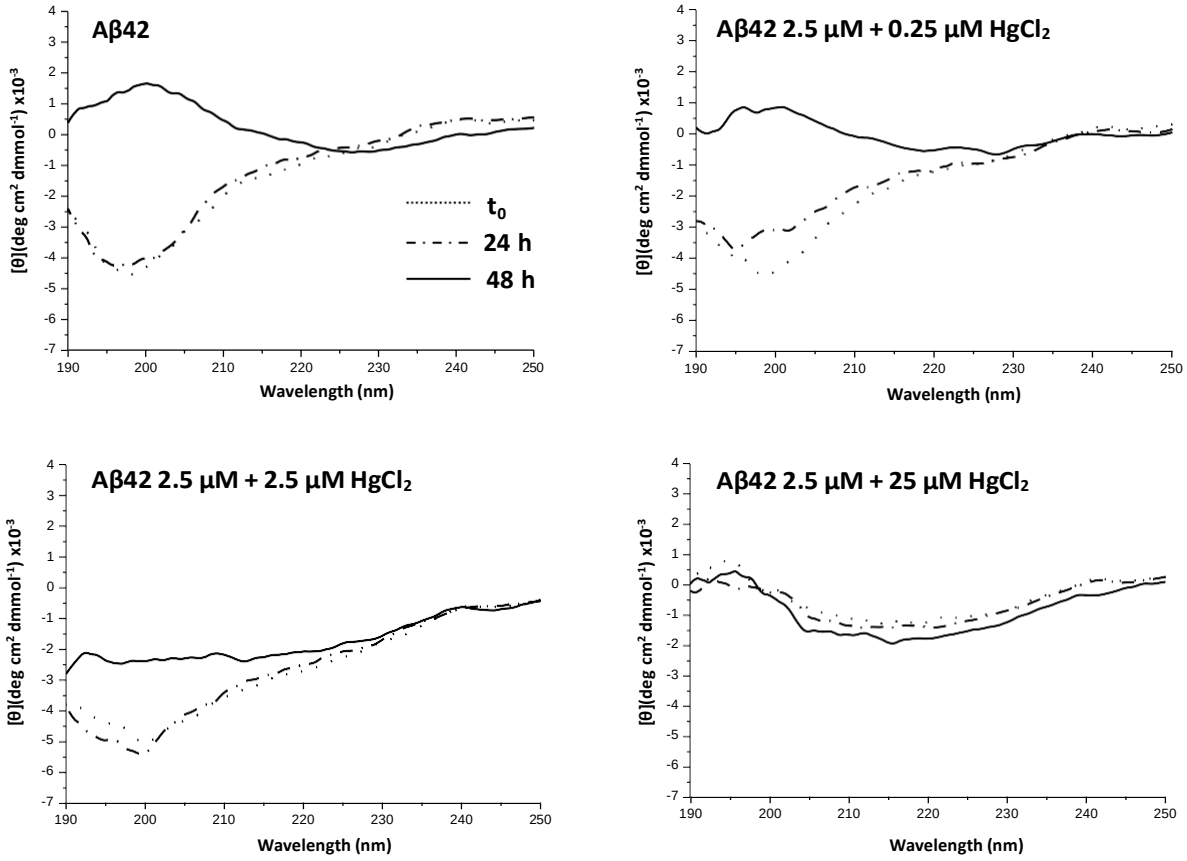
Aβ42
Aβ42 2.5 µM + 0.25 µM HgCl2
Aβ42 2.5 µM + 2.5 µM HgCl2
Aβ42 2.5 µM + 25 µM HgCl2
t0
24 h
48 h
[θ](deg cm2 dmmol-1) x10-3
Wavelength (nm)

Fig.4

Images

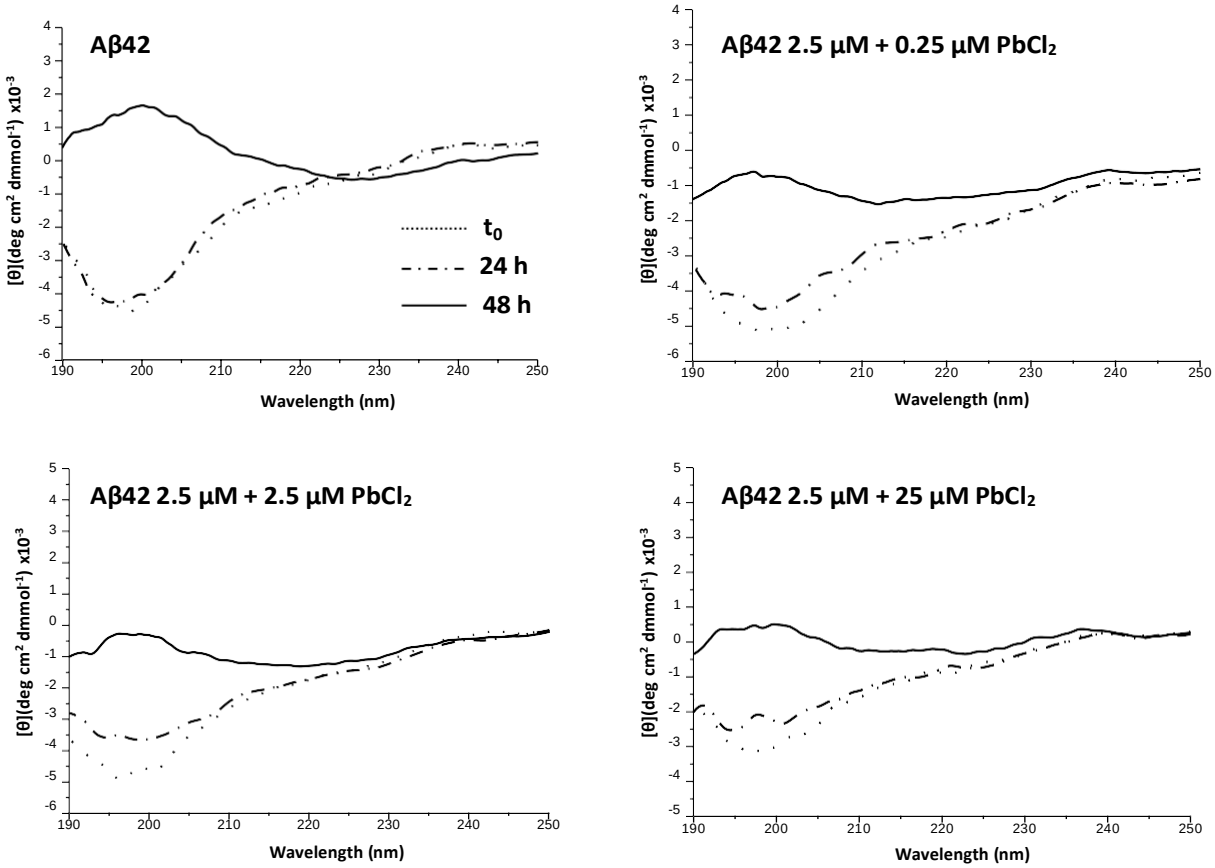
Aβ42
Aβ42 2.5 µM + 0.25 µM PbCl2
Aβ42 2.5 µM + 2.5 µM PbCl2
Aβ42 2.5 µM + 25 µM PbCl2
t0
24 h
48 h
[θ](deg cm2 dmmol-1) x10-3
Wavelength (nm)

Fig.5

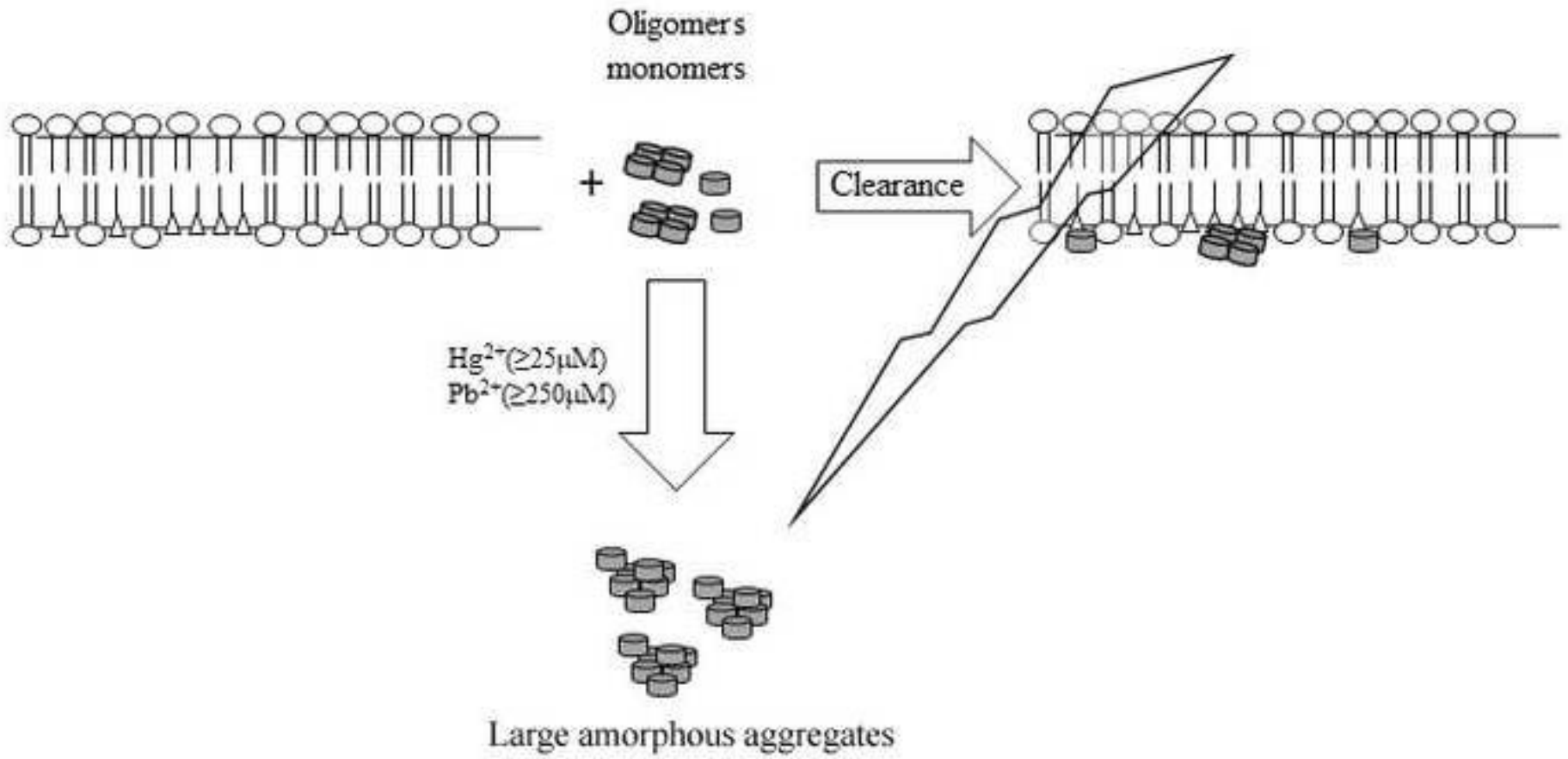

Fig.6